CONF-851115--43

Westinghouse Hanford Company

HEDL SA-3348 FP

RECEIVED BY OSTI DEC 18 1985

HEDL-SA--3348-FP

DE86 004015

TS-1 AND TS-2 TRANSIENT OVERPOWER TESTS ON FFTF FUEL

A. L. Pitner, P. C. Ferrell, G. E. Culley, E. T. Weber

October 3, 1985

American Nuclear Society
November 11, 1985
San Francisco, CA

U. S. Department of Energy

Assistant Secretary for Nuclear Energy
Office of Breeder Technology Projects
AF-15-40-10-2

HANFORD ENGINEERING DEVELOPMENT LABORATORY — Operated by the Westinghouse Hanford Company, P.O. Box 1970, Richland, WA, a subsidiary of the Westinghouse Electric Corporation, under U.S. Department of Energy Contract No. DE-AC06-76FF02170.

U.S. Department of Energy

DISCLAIMER

DISCLAIMER

TS-1 AND TS-2 TRANSIENT
OVERPOWER TESTS ON FFTF FUEL

A. L. Pitner, P. C. Ferrell, G. E. Culley, E. T. Weber

ABSTRACT

The TS-1 and TS-2 TREAT transient experiments subjected a low burnup (2 MWd/kg) and a medium burnup (58 MWd/kg), respectively, FFTF irradiated fuel pin to unprotected 5¢/s overpower transient conditions. The fuel pin failure response was similar in the two tests, which demonstrated a large margin to failure ($P/P_O > 3$) and a favorable upper level failure location. Thus, for these transient conditions, burnup effects on transient performance appeared to be minimal in the range tested. Pin disruption in the medium burnup TS-2 test was more severe due to the higher fission gas pressurization, but failure occurred at only a 5% lower power level than for the low burnup TS-1 fuel pin. Both tests exhibited axial extrusion of molten fuel to the region above the fuel column several seconds before pin failure, demonstrating a potentially beneficial inherent safety mechanism to delay failure and mitigate accident consequences.

TS-1 AND TS-2 TRANSIENT
OVERPOWER TESTS ON FFTF FUEL

A. L. Pitner, P. C. Ferrell, G. E. Culley, E. T. Weber

The TS-1 and TS-2 TREAT transient experiments were conducted on irradiated Fast Flux Test Facility (FFTF) fuel pins to characterize their failure behavior when subjected to hypothetical unprotected 5¢/s transient overpower conditions. The TS-1 test employed a near fresh (2 MWd/kg) fuel pin, while the TS-2 test used a medium burnup (58 MWd/kg) fuel pin. Transient conditions were closely matched in the two experiments to provide a direct comparison of burnup effects on the failure response.

The fuel pins tested were actual FFTF driver pins, consisting of a 0.914-m long column of mixed-oxide (22% PuO_2 / 78% UO_2) fuel contained in 5.84-mm diameter 20% cold worked Type 316 stainless steel cladding. The tests were performed in a Single Pin Test Loop (SPTL), shown schematically in Figure 1. The SPTL provided the appropriate thermal-hydraulic enrivonment for the test pins, while the TREAT reactor provided the desired nuclear environment. The loop assembly replaced the central two fuel elements in the TREAT core. Sodium coolant was pumped through the test train and recirculated by the Annular Linear Induction Pump (ALIP). Loop instrumentation included flowmeters, acoustic monitors, and thermocouples to measure sodium temperatures. The Argonne National Laboratory fast neutron hodoscope(1) was also used to monitor fuel motion in the tests. Simultaneous indications of pin failure were observed in all four types of sensors in each test. The reactor was programmed to scram immediately upon failure detection in each of the tests to preserve as much evidence as possible for post-test examination.

Each of the final TS-1 and TS-2 transient tests was preceded by a heat balance run to determine the power coupling between the reactor and the test pin. These runs consisted of constant power operation at

75% of steady state power and 100% flow (nominal power-to-flow ratio of 0.75) for 80 s, and in effect constituted calorimetry measurements wherein measured flow tube temperatures defined the heat deposition in each of the test pins. The temperature profiles measured during the heat balance runs are shown in Figure 2, along with the calculated temperatures using the Power Coupling Factors (PCF) indicated in the figure. The matchup between measured and calculated temperatures is seen to be quite good using the PCF's derived in this process. The lower PCF value for the TS-2 pin is due to burnup effects (depleted fissile content).

Applying the PCF's derived from the heat balance runs to the final transient runs gives the power histories presented in Figure 3. The overpower transient in each test was preceded by a 7 s flat-top period to simulate steady state thermal conditions in the fuel pin. At the 10 s mark, a power ramp simulating a 5¢/s reactivity insertion was initiated, and continued until pin failure occurred. It is seen that failure occurred at about the same time in each test pin. The TS-1 pin failed at 22.21 s into the transient, while the TS-2 pin failed at 23.83 s into the transient. Because it started at a lower steady state power level, the TS-2 pin actually failed at a slightly lower power level than the TS-1 pin, even though at a later point in the transient. The ratio of the pin power at failure to the steady state power was 3.1 for TS-1, and 3.4 for TS-2.

In spite of the large difference in burnup, there was only a 5% difference in pin power at failure for TS-2 and TS-1 (120 kW/m vs. 127 kW/m). Thus it would appear that the failure threshold for these types of fuel pins and transients is relatively insensitive to burnup level, at least up to about 60 MWd/kg. As indicated in Figure 3, failure occurred at an upper level in each pin (87% of the fuel column height for TS-1, and 72% of the fuel column height for TS-2).

Calculated flow tube temperatures during the final transients agreed well with measured values, as depicted in Figure 4. The indicated temperatures in the figure correspond to those at the end of each transient test, that is, at the time of failure. The excellent agreement between measured and calculated temperatures at the tops of the fuel columns indicates that the total integrated pin powers were properly accounted for in the analysis. The maximum flow tube temperature reached in the TS-1 test was 1310°K, while for the TS-2 test it was 1275°K. Cladding surface temperatures were on the order of 50°K hotter than adjacent flow tube temperatures near the end of the transient tests.

Following the TREAT transient testing, the test section of each loop assembly was neutron radiographed. These examinations verified that the test pins had failed, as evidenced by expelled fuel identifiable in the radiographs. The fuel pin disruption in TS-2 was significantly more severe than in TS-1. It was apparent that there had been extensive fuel melting in each of the test pins. An additional observation was that the fuel column had expanded axially in each test pin. Compared to pretest radiographs, the top of the TS-1 fuel column was elevated 1.7 cm, while the TS-2 fuel column was extended by 3 cm. These axial fuel extensions were detected by the hodoscope during the transient tests. The fuel movement in TS-1 occurred a full 5 s before pin failure, while in TS-2 it was observed 4 s before failure.

The TS-1 fuel pin was easily removed from the test train, due to the relatively minimal degree of disruption that occurred during the failure event. Figure 5 shows the cladding breach in this pin, located at X/L=0.87. The breach was quite small, less than 1 cm in length. A number of ceramography specimens were taken along the length of this test pin, and an assemblage of the micrographs obtained from these specimens is presented in Figure 6. The sections shown include a longitudinal specimen taken at the breach location, which depicts the fuel sweepout pattern. The transverse sections show the extensive fuel melting that occurred during the overpower transient. Based on the size of the central holes in these sections, it is estimated that about 25% of the fuel inventory in the TS-1 pin was expelled.

As indicated above, the cladding breach in TS-1 occurred at the X/L=0.87 level. However, a near-breach situation was found in a transverse section taken just above the primary breach. This is shown in Figure 7, which shows a cross section of the pin at the X/L=0.88 level. A radial crack is seen to have penetrated about 80% of the cladding wall at this point. The azimuthal location of the crack was opposite that of the primary breach. Thus, it appears that cladding breach may have been imminent at a number of separate upper level locations near the end of the transient.

The area of fuel relocation at the top of the fuel column in the TS-1 pin is shown in detail in the longitudinal micrograph presented in Figure 8. It is seen that molten fuel extrusion forced the two insulator pellets and axial reflector upward. The two insulator pellets were also separated slightly by the fuel extrusion. The total length of fuel extrusion seen here corresponds to the approximate free travel compression length of the plenum spring in this fuel pin. Thus, it appears that the upper pin components were lifted to the maximum extent possible by molten fuel extrusion; i.e., until the plenum spring was fully compressed. As noted previously, this event took place about 5 s before the pin failed. A similar occurrence apparently was detected by the hodoscope in the TS-2 test.

Such axial relocation of molten fuel can have significant safety implications. This phenomenon can serve to reduce internal pressurization loading on the cladding and accordingly delay its failure and the time at which molten fuel enters the coolant. Additionally, the relocation of fuel from the high worth central region of the fuel pin to the low worth end regions constitutes a negative reactivity feedback mechanism. If enough fuel were relocated in this manner, the consequences of such an unprotected overpower transient could be significantly mitigated, possibly even to the point of self-termination of the accident. In this respect, it would appear desirable to provide appropriate space and pathways for axial fuel relocation in the design of Liquid Metal Reactor (LMR) fuel pins.

The TS-2 test pin was found to be highly disrupted in the upper levels, and removal from the flow tube proved to be quite difficult. Only the portion below the X/L=0.59 level was recovered for examination. The fuel pin was severely disrupted from X/L=0.71 to X/L=0.82. The radiograph indicated that there were intact fuel pellets in the upper levels of the pin, but the cladding was found to be melted away all the way to the top of the fuel column. The free standing fuel pellet shells remaining in the upper levels were dispersed during disassembly operations.

Fuel melting in the TS-2 pin was found to be extensive, similar to TS-1. As indicated above, no specimens were obtained in the upper levels of the TS-2 fuel pin, but the melt fractions at the lower levels agreed with the TS-1 observations. Figure 9 shows comparative cross section views of transverse ceramography specimens taken near the midplane of both test pins. It is seen that the degree of fuel melting is about the same in the two pins at this level (77 areal %), but the TS-2 pin shows a substantially larger central hole. This was typical of all specimens examined. Based on ceramography and neutron radiography observations, it is estimated that more than half of the TS-2 pin fuel inventory was expelled during the failure event.

The diameters of a number of sections removed from each fuel pin were measured using hot cell mensuration equipment. These diameters were compared to pretest profilometry traces to determine if any transient induced cladding strain had been incurred. The below midplane sections recovered from the TS-2 pin showed no cladding strain. Similarly, no positive cladding strain was observed in lower level TS-1 pin sections. However, definite strain was noted in upper level TS-1 sections, as shown in Figure 10. There is significant error in the hot cell diameter measurements, and the strain band shown in the figure reflects this measurement uncertainty. Cladding strain in this pin was found to increase from zero near the midplane to greater than 1% at the highest level measured (X/L=0.93). This strain profile is typical of that induced by internal pressurization, with the increasing strain toward the top reflecting the reduced cladding strength associated with the higher coolant temperatures in this direction.

Post-test modeling of the experiments was performed using the TEMECH fuel pin transient analyis code. These evaluations showed that both fuel pins failed from internal pressurization. In the case of TS-1, which tested a low burnup pin with little fission gas content, the major contributor to the pressurization process was molten fuel expansion. While this also played a role in the TS-2 fuel pin failure, the principal pressurization source in the failure process here was release and heatup of the greater inventory of fission gases. The analyses also indicated that the molten fuel extrusion that occurred 4 to 5 seconds before failure delayed the timing of the failure event by about 1 s in each of the test pins.

The principal conclusions that can be drawn from these test results are:

1. Large margins to failure were demonstrated by these FFTF reference fuel pins. They survived more than 20 seconds into the 5¢/s overpower transient to power levels more than three times nominal steady state levels before failing, whereas the FFTF plant protection system would scram the reactor after approximately 3 s at 25% maximum overpower under these transient conditions.

2. Failure timing for these types of fuel pins and transients appears to be relatively insensitive to fuel burnup, at least up to about 60 MWd/kg.

3. The cause of failure in each test was internal pressurization. The principal pressurization source in the low burnup TS-1 pins was molten fuel expansion, while for the medium burnup TS-2 pin it was fission gas release and heatup.

4. Pre-failure axial molten fuel relocation was observed in both tests, demonstrating a potential inherent safety mechanism.

Reference

1. A. DeVolpi, et al., "Fast-Neutron Hodoscope at TREAT: Methods for Quantitative Determination of Fuel Dispersal," Nucl. Tech. 56, p. 141.

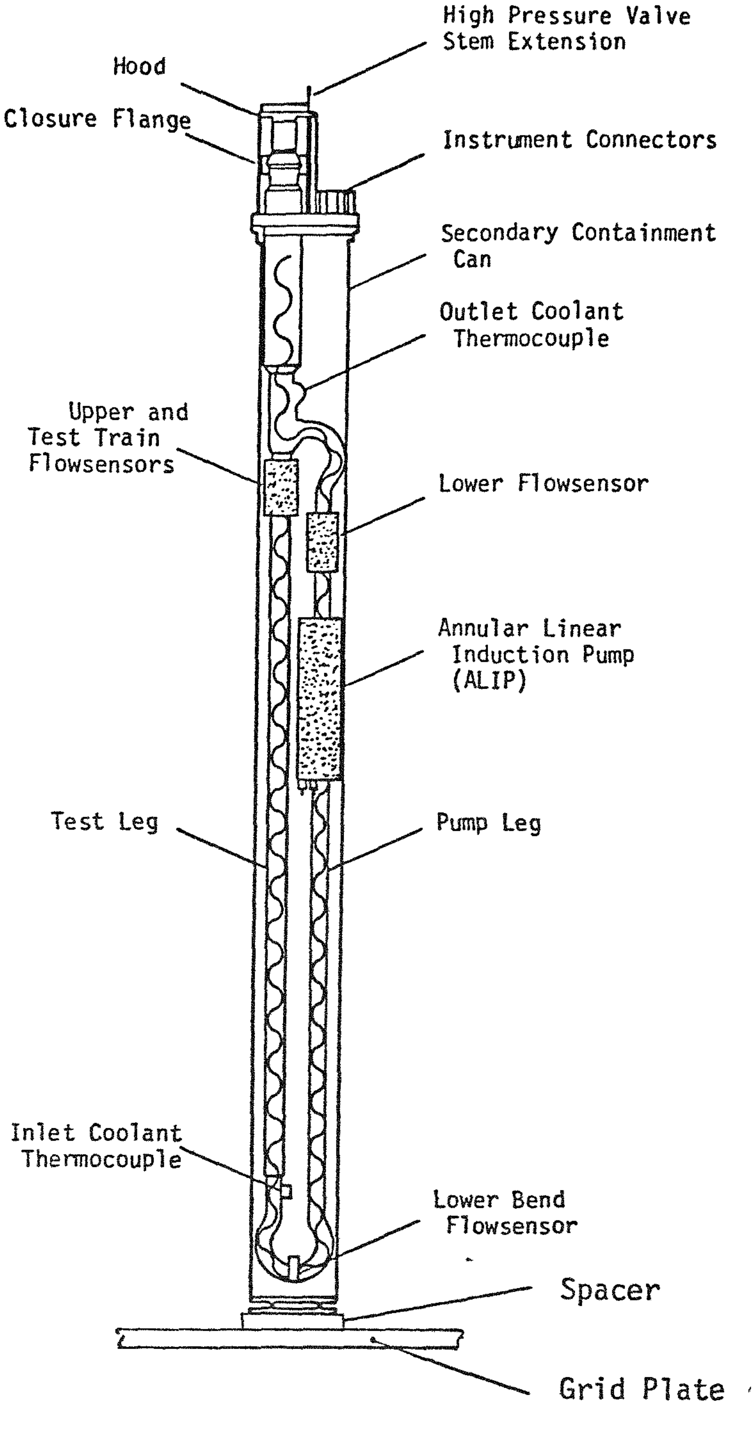

FIGURE 1. Single Pin Test Loop

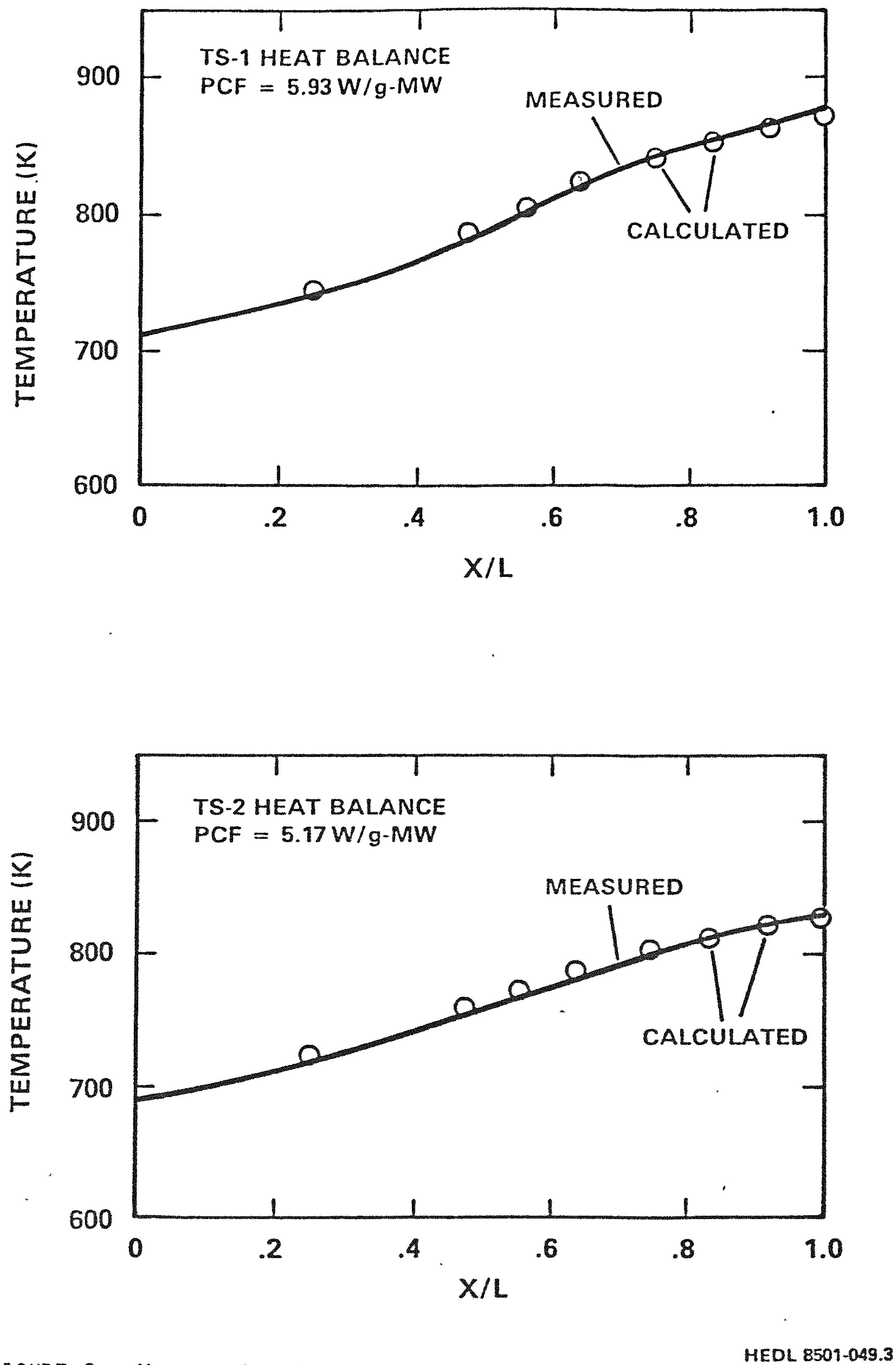

FIGURE 2. Measured and Calculated Flow Tube Temperatures During Heat Balance Runs

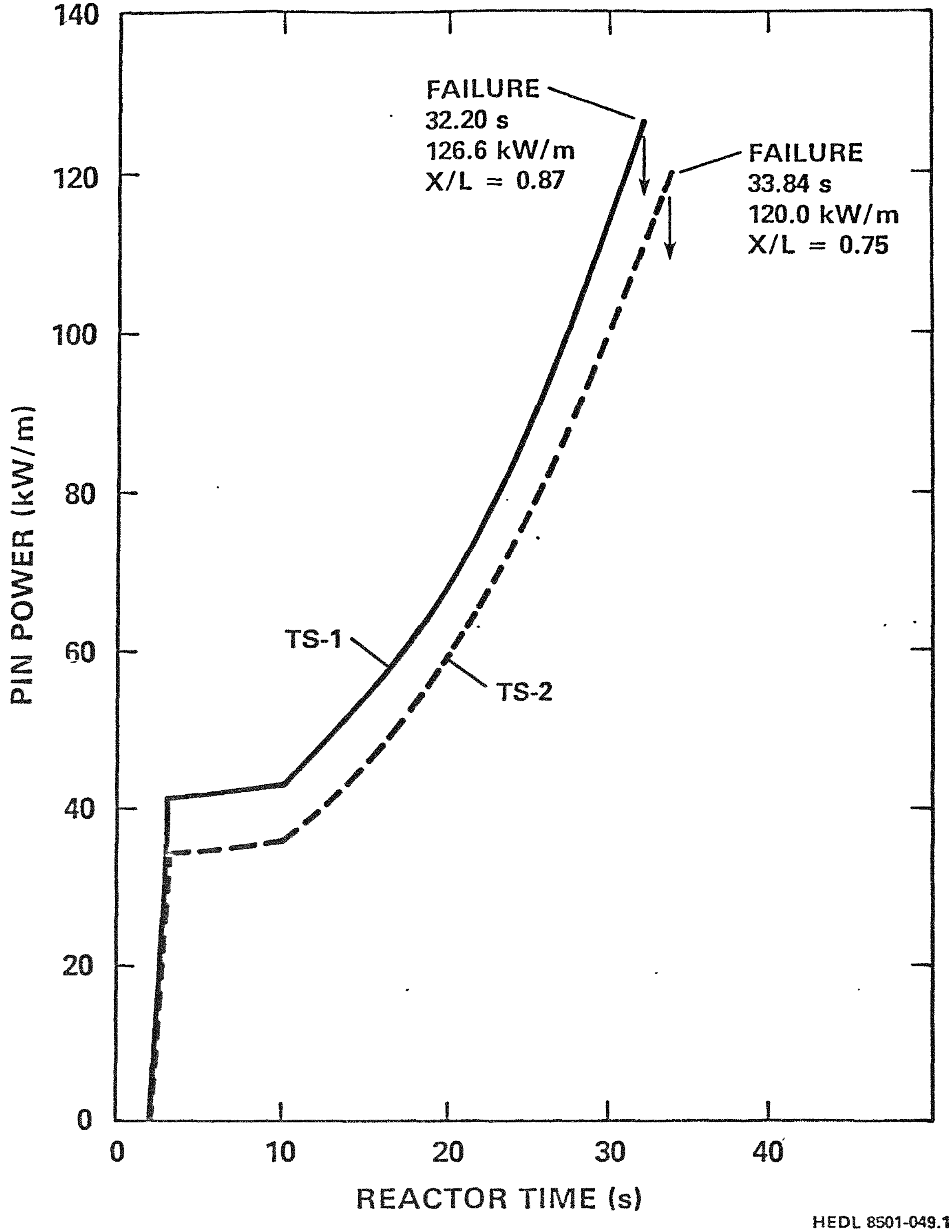

FIGURE 3. Final Transient Power Histories

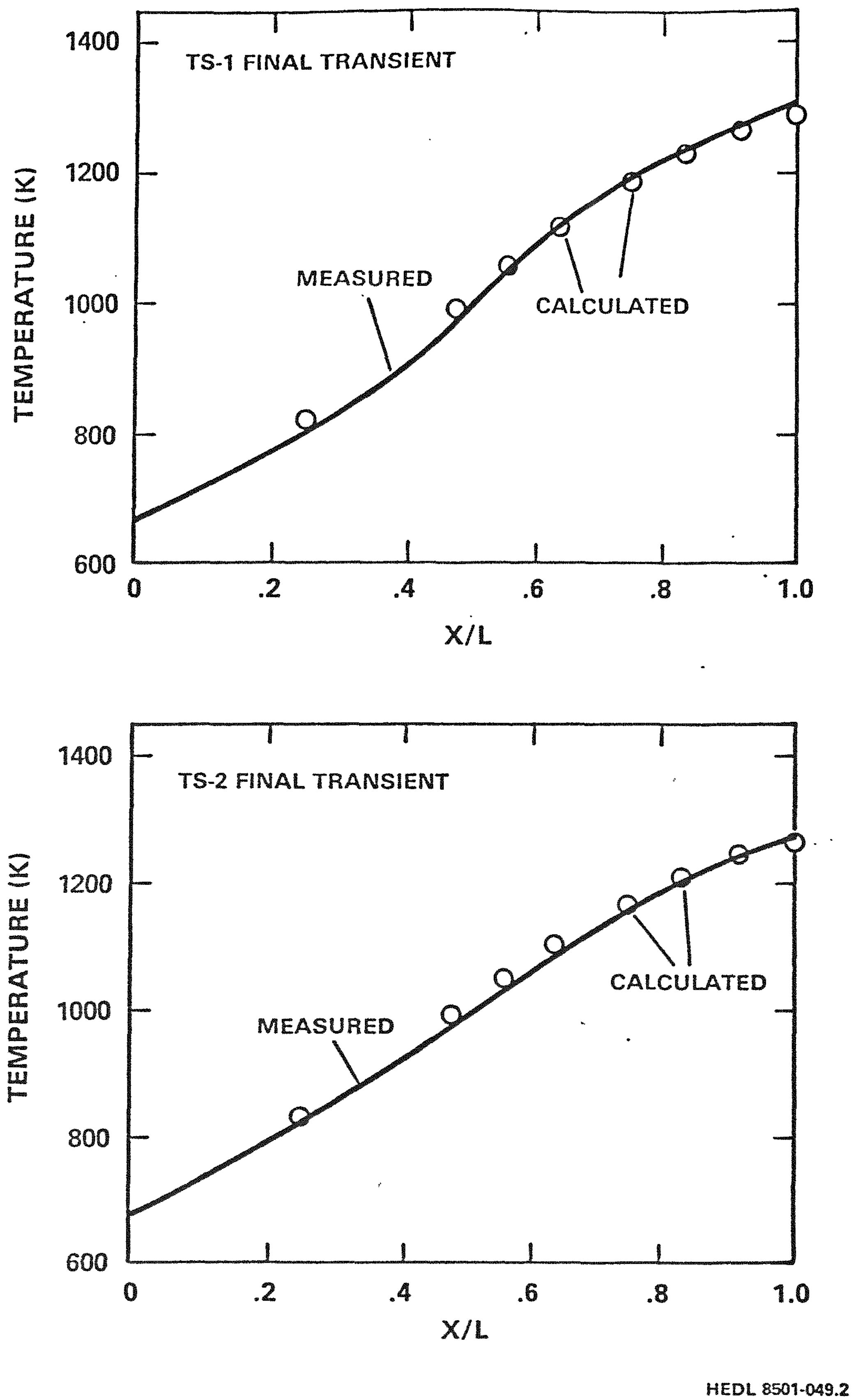

FIGURE 4. Measured and Calculated Flow Tube Temperature Profiles at Pin Failure Time

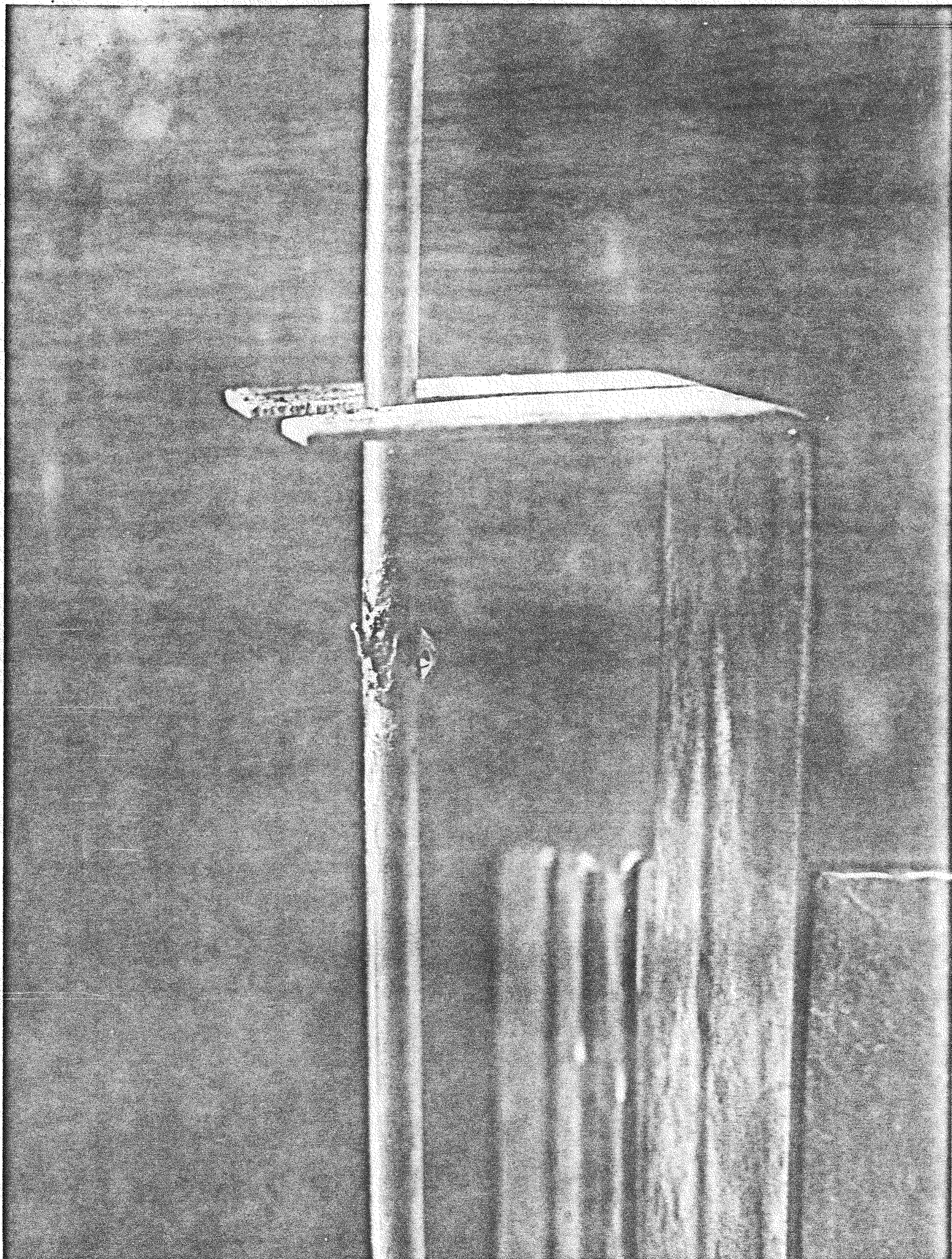

FIGURE 5. TS-1 Cladding Breach (X/L = 0.87)

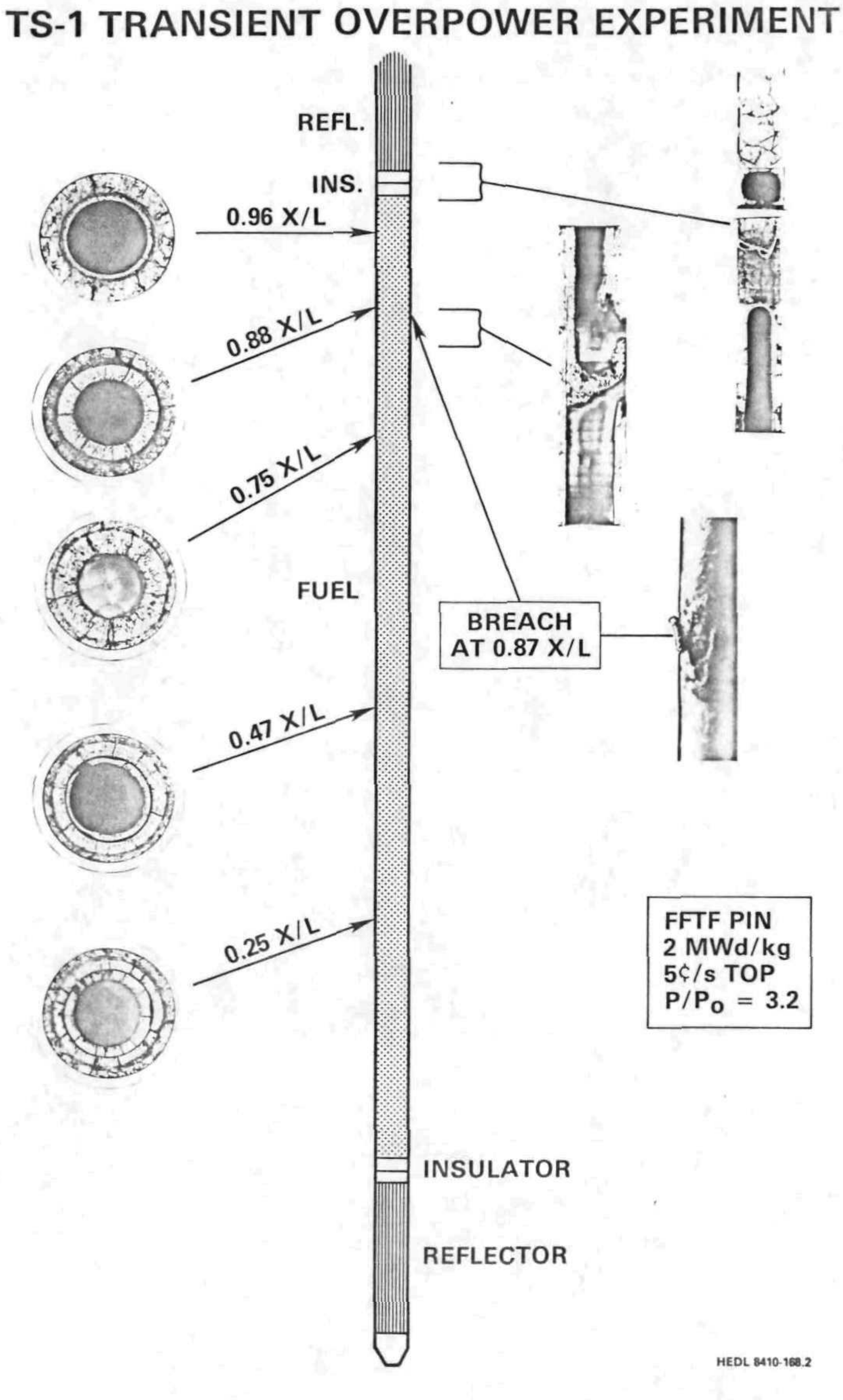

FIGURE 6. TS-1 Ceramography

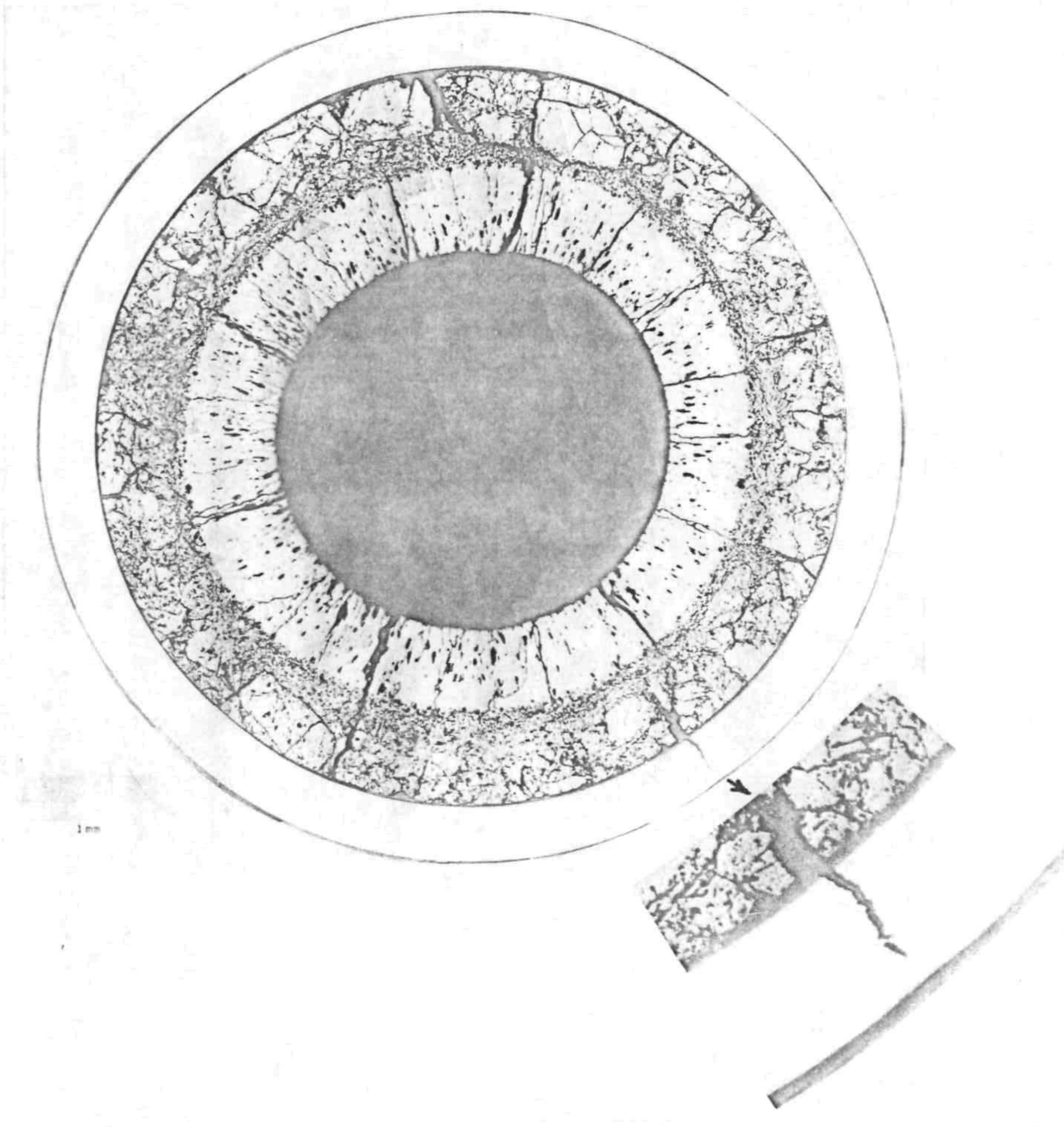

FIGURE 7. Near-Breach in TS-1 Pin (X/L - 0.88)

TS-1 MOLTEN FUEL RELOCATION

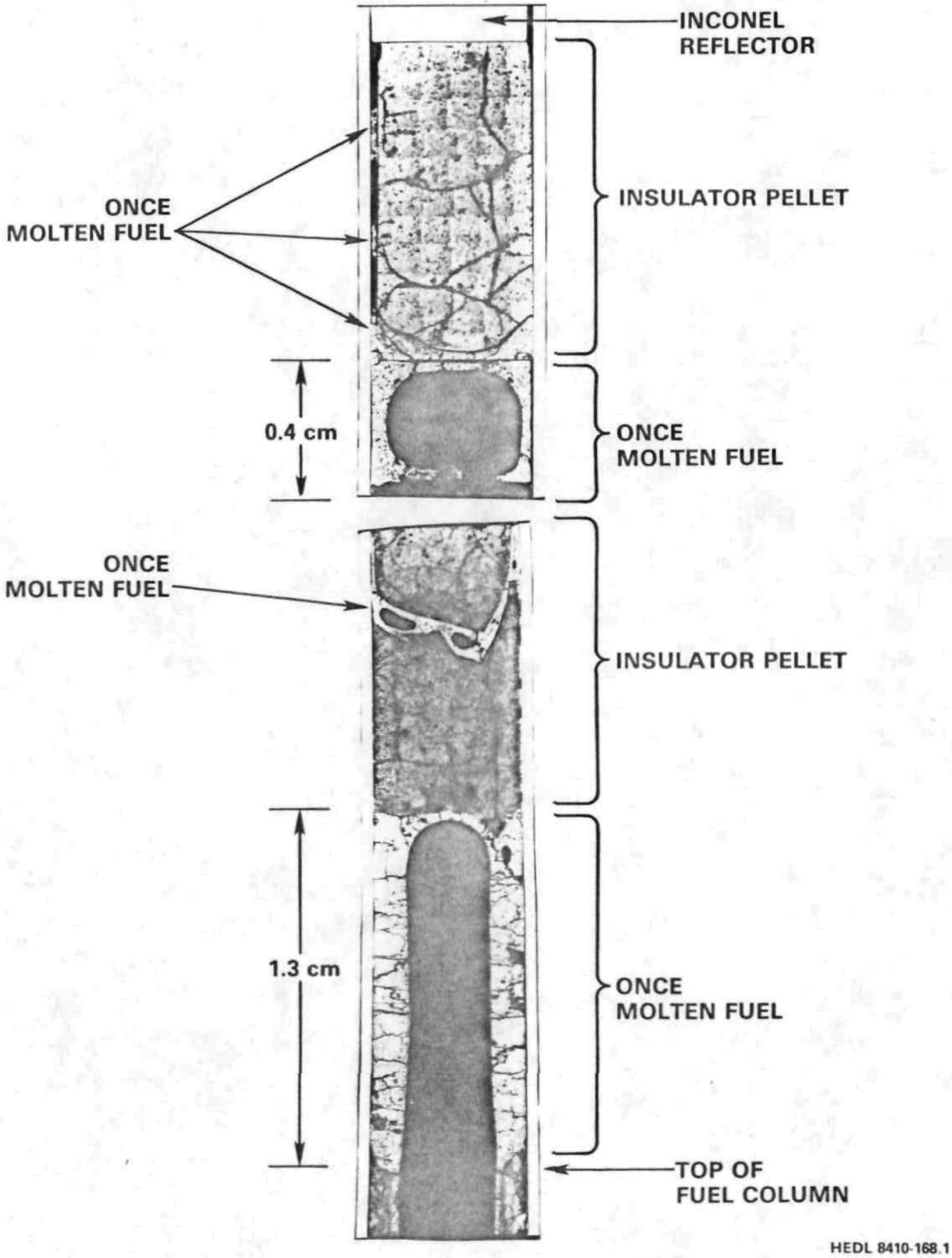

FIGURE 8. TS-1 Molten Fuel Relocation

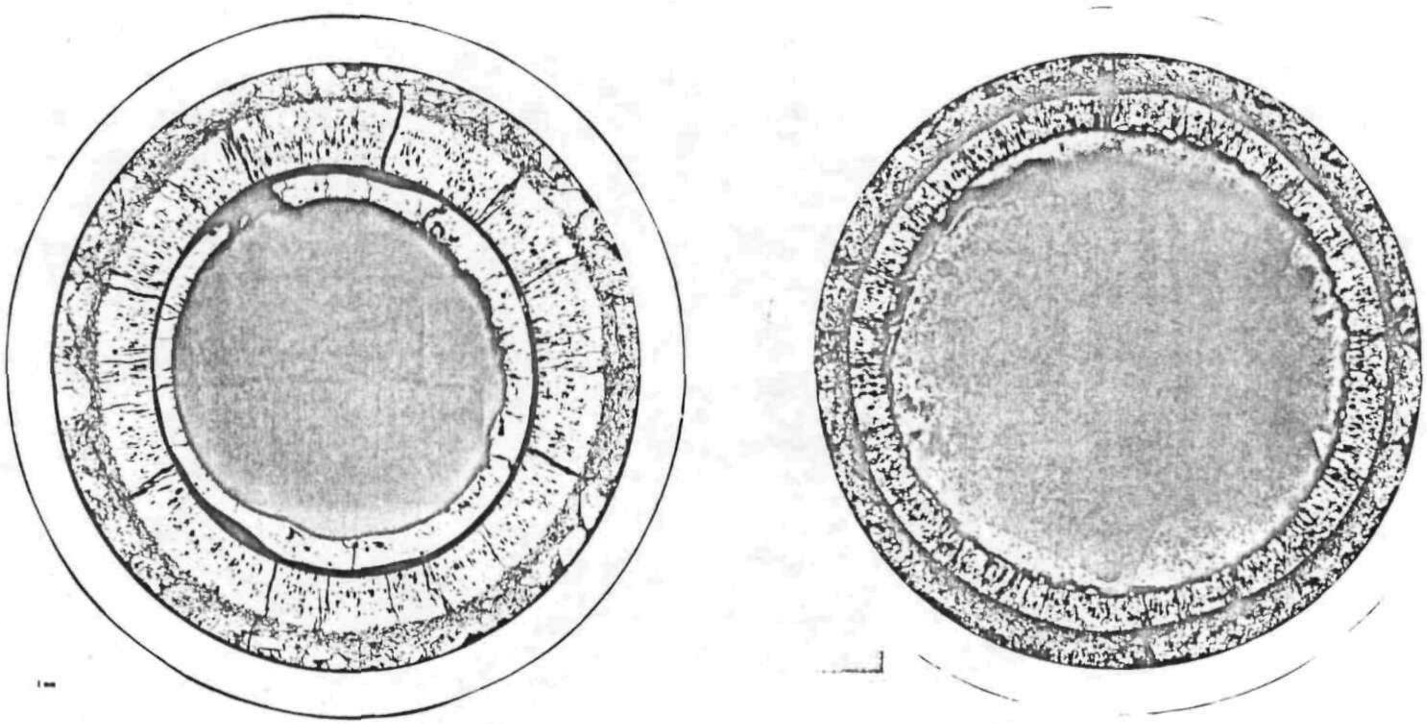

FIGURE 9. Transverse Ceramography Sections (X/L = 0.47)

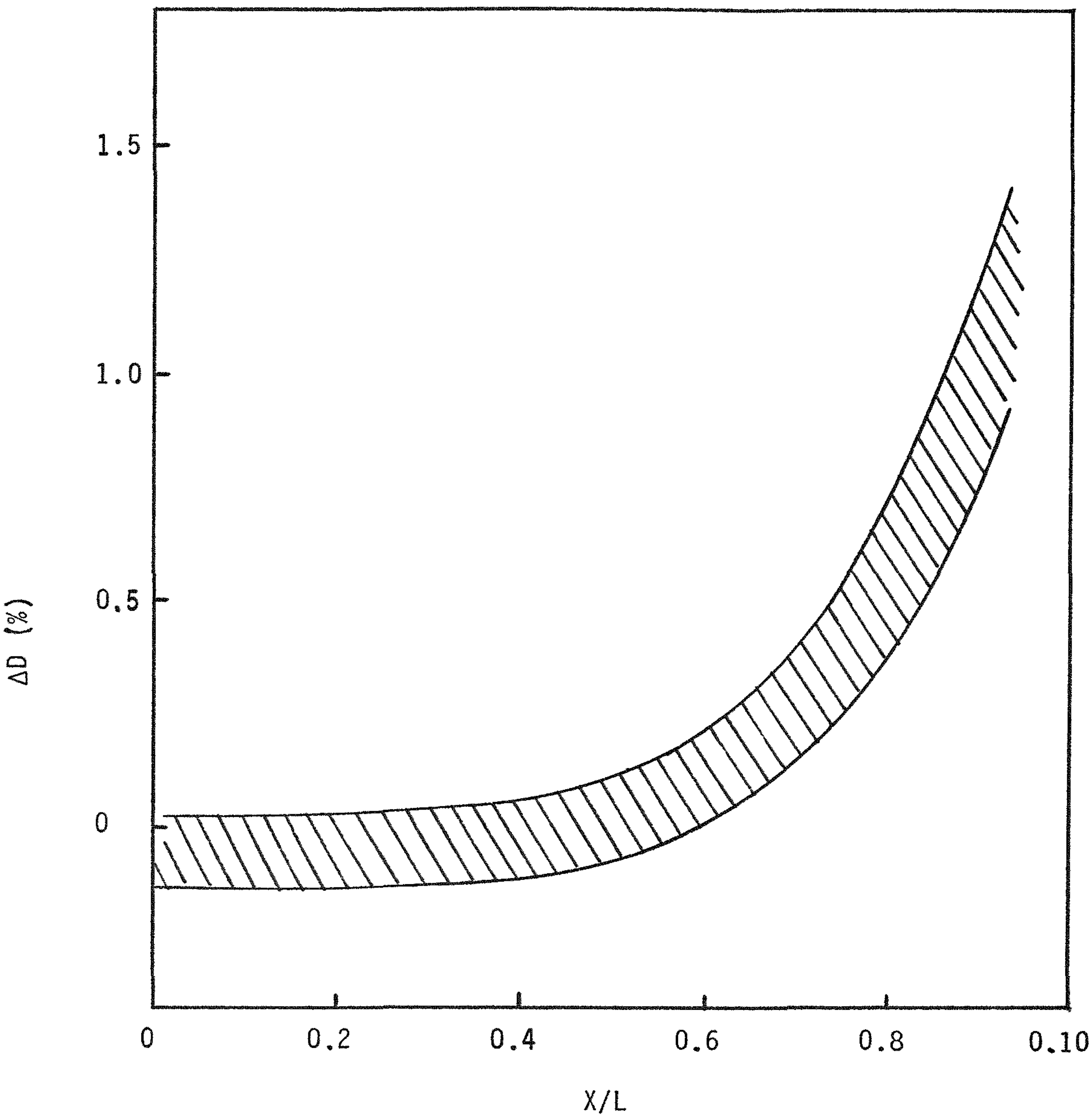

FIGURE 10. TS-1 Cladding Strain